Original Article

A New Hypothesis on the Frequency Discrimination of the Cochlea

Erdoğan Bulut, Cem Uzun, Levent Öztürk, Pınar Turan, Mehmet Kanter, Serap Arbak

Department of Audiology, Trakya University Faculty of Health Sciences, Edirne, Turkey (EB)
Department of Otorhinolaryngology, Trakya University School of Medicine, Edirne, Turkey (CU)
Department of Physiology, Trakya University School of Medicine, Edirne, Turkey (LÖ, EB)
Center of In-vitro Fertilization, Marmara University School of Medicine, İstanbul, Turkey (PT)
Department of Histology and Embryology, İstanbul Medeniyet University School of Medicine, İstanbul, Turkey (MK)
Department of Histology and Embryology, Acıbadem University School of Medicine, İstanbul, Turkey (SA)

OBJECTIVE: Medial olivocochlear efferent (MOCE) neurons innervate outer hair cells (OHCs) of the cochlea, which in turn leads to basilar membrane motion. We hypothesized that MOCE-induced alterations in basilar membrane motion, independent of traveling waves, is responsible for the cochlear frequency discrimination of sound.

MATERIALS and METHODS: Eleven guinea pigs underwent bilateral otoscopic and audiologic evaluations under general anesthesia. The study comprised two parts. Part I (n=11) included spontaneous otoacoustic emission (SOAE) recordings with or without contralateral pure-tone acoustic stimuli (1 and 8 kHz) at 60 dB sound pressure level (SPL). Part II involved pure-tone (1 or 8 kHz) acoustic trauma in the right ears of two randomly selected subgroups (G1: 1 kHz; n=4 and G8: 8 kHz; n=4). The remaining three animals served as controls. After frequency-specific deafness was confirmed by distortion product otoacoustic emission (DPOAE), SOAEs were recorded in the left ears in the presence of a contralateral pure-tone (1 and 8 kHz) stimulus of 60 dB SPL. Furthermore, the surface of the organ of Corti was examined by scanning electron microscopy (SEM).

RESULTS: The contralateral pure tone led to frequency-specific activation in SOAEs in part I (without trauma) and part II (with trauma) measurements. SEM showed heterogeneous OHC damage along the cochlea in traumatized ears with pure tone.

CONCLUSION: We suggest that MOCEs convey acoustic information from traumatized ears to intact ears. Traumatized ears can show frequency-specific activation in the presence of diffuse damage in OHCs that excludes the passive transmission of the pressure wave from the perilymph to the basilar membrane.

KEYWORDS: Efferent pathways, cochlear outer hair cells, otoacoustic emissions, spontaneous, basilar membrane, microscopy, electron, scanning

INTRODUCTION

The pitch perception and sound processing function of the cochlea are explained by the traveling wave theory proposed by von Bekesy [1]. According to the theory, different frequencies of sound lead to peak vibrations in different places on the basilar membrane. Low frequencies cause greatest vibrations around the apex, whereas high frequencies elicit greatest vibrations around the base of the cochlea. Electrical measurements reveal that hair cells in different regions in the cochlea respond to different frequencies of a sound stimulus [2]. Accordingly, a tonotopic map was identified in the cochlea [3]. The traveling wave is amplified and sharpened through a process called cochlear amplification. Outer hair cells (OHCs) are at the very center of cochlear amplification and frequency selectivity [2, 3]. When OHCs lying on a certain region of the basilar membrane become active, the corresponding frequency component of sound can be perceived. Thus, the frequency discrimination of cochlea can be explained by the traveling wave theory.

However, it is obvious that the traveling wave theory cannot adequately explain some morphological and functional observations reported in the literature. For instance, OHC length differs along the basilar membrane [4]. OHCs around the base are shorter, whereas OHCs around the apex are taller. If the main factor is the passive vibration of the basilar membrane with a traveling wave, there is no need for the different morphology of OHCs. Von Bekesy's traveling waves were measured in cadavers, but we now know that in

living mammals, the mechanical properties of the basilar membrane are not linear. Finally, if the theory is correct, it should be possible to create frequency-specific hearing loss when a pure tone is applied at very high sound-level intensities such as 120 dB sound pressure level (SPL). In that case, an ultrastructural examination of the cochlea with frequency-specific hearing loss should demonstrate regional, rather than diffuse, damage of OHCs.

The contraction and relaxation properties of OHCs may play a significant role in discriminating different frequency bands in the cochlea [5]. The discovery of a motor protein, called prestin, that is present on the lateral membrane of OHCs supports this opinion [6, 7]. The medial olivocochlear efferent (MOCE) branch synapses with OHCs, and the efferent pathway can be activated via electricity or a sound stimulus [8]. In other words, while it was previously thought that only sensory information is carried from OHCs to auditory signal pathways, it is now known that some neural signals are received by OHCs as efferent innervation and affect OHC function. For instance, the activation of medial efferents can change OHC motile responses [9] and convert signals that are capable of controlling the sensitivity of the peripheral hearing system in a frequency-specific manner [8]. Frequency discrimination might not be due to basilar membrane motility but might occur as a reflex activation. This reflex activation, which is unique in all cochlear segments, can be achieved with inner hair cells (IHCs) and OHCs and their reflex connections. The neural activation of MOCE can play a key role in this frequency discrimination along with OHCs, and the basilar membrane creates a vibration pattern for OHCs.

In light of the above considerations, we conducted the present study to test von Bekesy's traveling wave theory, and we hypothesized that the frequency discrimination of the cochlea is not dependent on the maximal vibration of a traveling wave; rather, it is dependent on the primary electromotile properties of OHCs. We planned to create frequency-specific hearing loss using a pure-tone stimulus at harmful levels (i.e., 1 and 8 kHz, 120 dB SPL for 20 min). All animals showed frequency-specific hearing loss that was verified by distortion product otoacoustic emissions (DPOAEs). After the verification of hearing loss, all animals were decapitated and the preparations of cochlea were examined by scanning electron microscopy (SEM).

MATERIALS and METHODS

Animals
After obtaining the approval of the local ethics committee, 11 healthy young adult pigmented guinea pigs (weight range, 300–600 g) with normal auropalpebral reflexes were used. All animals underwent a bilateral otoscopic examination and an audiologic evaluation, including 1 kHz probe-tone tympanometry and auditory brainstem response (ABR) and otoacoustic emission (OAE) tests. Tympanometric and all OAE measurements were performed with a Madsen Capella (GN Otometrics A/S, Taastrup, Denmark) OAE device. The probe assembly was fixed with an adaptor to allow tight and deep insertion into the ear canals of the guinea pigs, and the probe was fixed in an appropriate position with a holder during the measurements. The animals were placed in a sound-attenuated chamber. All measurements were performed with the guinea pigs under general anesthesia achieved by an intramuscular injection of ketamine (40 mg/kg) and xylazine (10 mg/kg). Their body temperature was maintained at 38°C with a warming blanket. Eleven guinea pigs with normal findings in tympanometry, DPOAE, and ABR tests were randomly divided into pure-tone acoustic trauma groups G1 (1 kHz; n=4) and G8 (8 kHz; n=4) and a control group (n=3). The study comprised two parts. Part I (n=11) included spontaneous OAE (SOAE) recordings with or without contralateral (CL) pure-tone acoustic stimuli (1 and 8 kHz) at 60 dB SPL. Part II involved the same animals with pure-tone (1 or 8 kHz) acoustic trauma in the right ears of two randomly selected subgroups (G1, n=4 and G8, n=4). The remaining three animals served as controls.

Audiologic Evaluation

Tympanometric examination
The probe tone was set at 1 kHz; the pump speed was 100 daPa/s, and the pressure range of measurement was set at +200 to −200 daPa. Type "A" tympanograms (peak pressure: between +100 and −100 daPa) were accepted as normal.

SOAE measurements
Input sensitivity was 0–70 dB SPL; the equalized output of the system was flat (±5 dB) from 0.5 to 10 kHz. The microphone output was amplified, and the response was subjected to spectral analysis. The SOAE sampling was based on averages of 500 accepted sweeps for the purpose of noise reduction. The grand average was calculated, and the results were displayed. SOAE was considered present if the SOAE was at least 5 dB above the noise floor and the spectral peak could be suppressed by an external acoustic tone. It was also characterized in terms of amplitude (dB SPL) and frequency (Hz). SOAEs were visually identified as narrow peaks in the frequency spectrum and via a cursor function.

DPOAE measurements
Acoustic stimuli were two continuous pure tones at the so-called primary frequencies f_1 and f_2. The primary levels L_1 and L_2 were separately adjusted, and their frequency ratio f_2/f_1 was fixed at 1.22. Stimulus levels were fixed at L_1=65 and L_2=55 dB SPL. The DPOAE measurement was evaluated when the generation of the $2f_1$-f_2 DPOAE occurred by primaries with geometric mean frequencies between 0.75 and 8 kHz. The testing time was 60 s. A common criterion for confirming the detection of DPOAE is that its amplitude must be at least 3 dB above the average level of the noise floor sampled at several frequencies surrounding the emission frequency [10]. Frequency-specific signal/ noise ratios (S/N-R) were observed in both ears of the guinea pigs.

ABR measurements
Auditory brainstem responses were recorded by three silver needle electrodes that were subdermally placed over the vertex (positive), ipsilateral mastoid (negative), and contralateral mastoid (ground/ reference) of guinea pigs. Click stimuli (duration: 0.1 ms; frequency bandwidth: 1–4 kHz) were delivered through an E-A-R Tone 3A (Aearo Co, Indianapolis, IN) insert earphone, and ABR was recorded using BRA2-05/95 version 5.XX (Danplex, Neckartenzlingen, Germany). The repetition rate was 10/s, and an average of 300 sweeps was recorded. The stimulus intensity was 80 dB SPL initially, which was followed by 10 dB decrements until waveforms were no longer present, thus determining the threshold of ABR. The ABR threshold was defined as the lowest dB SPL level that produced a reliable peak III in the ABR waveforms.

Pure-tone contralateral acoustic stimulus and acoustic trauma
Pure-tone CL acoustic stimuli and high-intensity stimuli were generated with the same audiometer (Interacoustic Diagnostic Audiometer AD-17, Assens, Denmark) to induce acoustic trauma and were delivered through a small transducer connected to the appropriate ear canal via E-A-R Tone 3A insert earphones. CL pure-tone stimulus intensities of 60 dB SPL during the testing time at 1 or 8 kHzwere generated by the audiometer. The G1 and G8 groups were exposed to a pure-tone stimulus of 120 dB SPL for 20 min at either 1 or 8 kHz to induce acoustic trauma. The control group was exposed to the CL stimulus without acoustic trauma. Frequency-specific deafness was confirmed by DPOAE, and acoustic trauma was induced according to the method described and confirmed by Uzun et al. [11].

Ultrastructural Evaluation

Scanning Electron Microscopy
After decapitation, the temporal bones were stored with 2.5% glutaraldehyde in a 0.1 M phosphate buffer for 12 h and then rinsed with a 0.1 mL/L phosphate buffer at pH 7.4 for 1 day. After incubation in a 0.1 M Sodium-Ethylenediaminetetraacetic acid (Na-EDTA, Sigma, Germany) decalcifier (pH 7.4) for 2 weeks, the tympanic bulla of the temporal bones (Figure 1) was opened and the otic capsule of the cochlea (Figure 2) was removed under a microscope. The cochlea was post-fixed with 1% osmium tetroxide in the phosphate buffer for 1 h and then rinsed with the phosphate buffer. Tissues were dehydrated through a graded series of ethanol and were then dried with amylacetate in a critical point dryer (CPD 010; Balzer Union, Liechtenstein) and sputter-coated with gold palladium in a Bio-Rad-SC502 sputter coater (Hemel Hempstead, Herts, UK). The surface topography of the organ of Corti was examined and photographed with a scanning electron microscope (JSM-6335F; JEOL, Tokyo, Japan). In the examination, the terms "rows" and "segments" were used to describe OHC stereocilia damage. "Rows" were used to indicate horizontal alignment, and "segments" were used to indicate vertical alignment.

Statistical Analysis
Descriptive statistics was used. Normal distribution was tested by Kolmogorov–Smirnov analysis. Due to the limited number of animals in the groups, non-parametric tests were used. Intragroup comparisons were made by the Wilcoxon test, and intergroup comparisons were made by the Kruskal–Wallis test.

RESULTS

Part I

SOAE recordings (before and after acoustic stimulus)
Before the acoustic stimulus, the SOAE scores were approximately 9 kHz in the control, G1, and G8 groups (Figure 3). SOAE scores were also recorded after the CL acoustic stimulus (right ear: CL stimulus; left ear: recording) with frequency-specific stimulation (Figure 3) signals (G1: 1 kHz and G8: 8 kHz). An additional SOAE record (different amplitude) was obtained before the acoustic stimulus besides the SOAE records obtained during the contralateral acoustic stimulus (Figure 3). While minimum responses were recorded at other frequency bands, SOAE amplitudes measured maximum responses to stimuli at a given frequency band.

Figure 1. The cochlea in the tympanic cavity (Magnification 15×1.5×11.2)

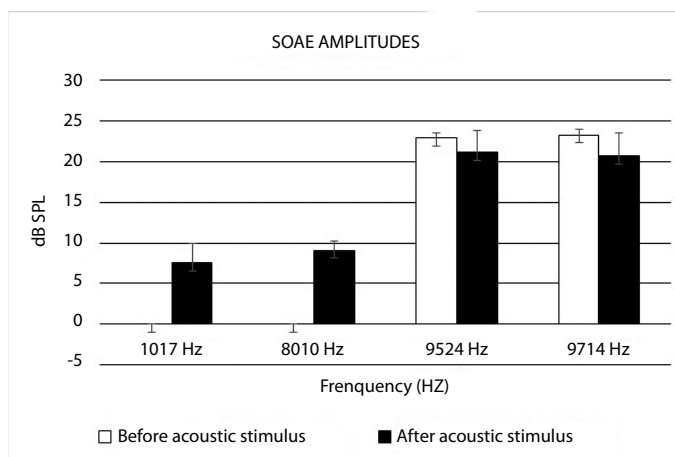**Figure 2.** Modiolus (Magnification 15×1.5×11.4)

Figure 3. The mean amplitudes of SOAE in the groups.
SOAE: spontaneous otoacoustic emission

Part II

DPOAE recordings (before and after acoustic trauma)
The S/N-R in the DPOAE tests at all frequency levels in the control groups were greater than 3 dB. They increased from lower to higher
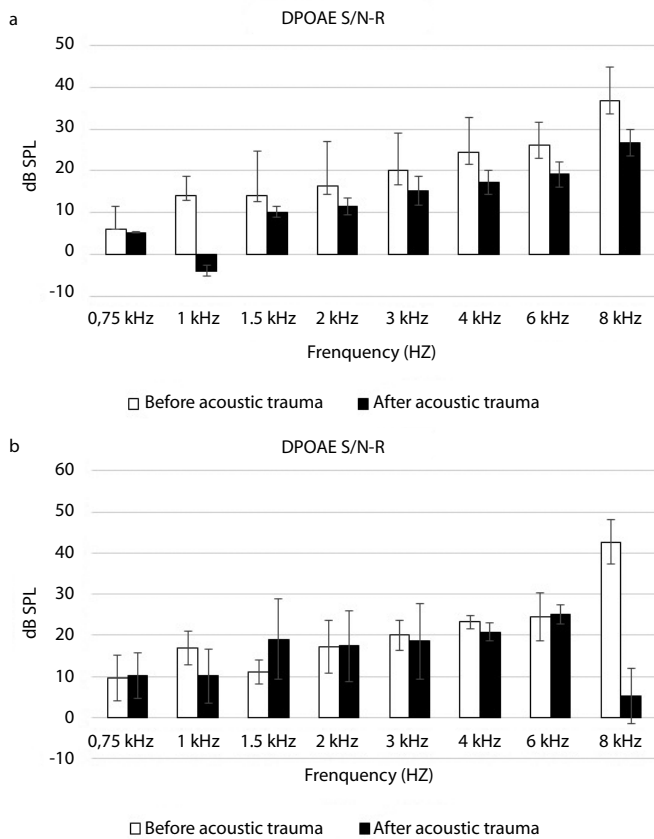
a

DPOAE S/N-R

b

DPOAE S/N-R

Figure 4. a, b. The mean of S/N-R DPOAE in the G1 (a) and G8 (b) groups.
DPOAE: distortion product otoacoustic emission

a

SOAE AMPLITUDES

□ Before Acoustic Trauma CL (-)   ■ Before Acoustic Trauma CL (+)
▨ After Acoustic Trauma CL (+)

b

SOAE AMPLITUDES

□ Before Acoustic Trauma CL (-)   ■ Before Acoustic Trauma CL (+)
▨ After Acoustic Trauma CL (+)

Figure 5. a, b. The mean of amplitudes SOAE in the G1 (a) and G8 (b) groups.
SOAE: spontaneous otoacoustic emission

frequencies depending on the motility of OHCs located on the co-chlea. Acoustic trauma was created in the right ears that were stimu-lated by the contralateral acoustic stimulus with a specific frequency (G1: 1 kHz and G8: 8 kHz). At 1 and 8 kHz, the S/N-R of the trauma-tized ears dramatically decreased (Figure 4a, b).

SOAE recordings (after acoustic trauma)
The OHC responses of the right ears that underwent CL stimulus were inhibited by the acoustic trauma. After the acoustic trauma, frequency-specific varying amplitudes responses were found in the ipsilateral SOAE recordings (left ear) from the CL stimulus giv-en to the right ears (Figure 5a, b) in the G1 and G8 groups, respec-tively.

Ultrastructural assessment
Following the examination of the surface topography of the organ of Corti to evaluate OHC stereocilia morphology, no degeneration was observed in the control group (Figure 6). The morphological damage of OHCs along the basilar membrane was heterogeneous rather than region-specific. In other words, OHC damage in the G1 (Figure 7) and G8 (Figure 8a, b) groups was comparable. In the frequency-specific acoustic trauma, damage of the basilar membrane segments that showed maximum vibration was expected. No degeneration result-ing from a different point of maximum vibration injury in the same segment of OHC (I, II, and III rows) stereocilia damage was observed. The ultrastructure of OHCs after acoustic trauma showed a heteroge-neous involvement. For instance, one OHC in a row appeared totally abolished, while the adjacent cell appeared entirely normal. The dis-
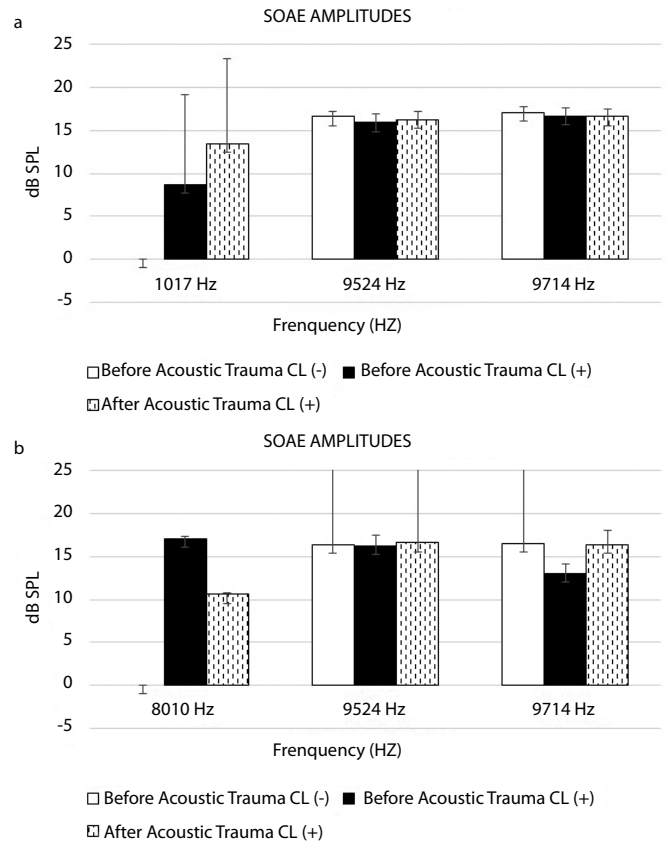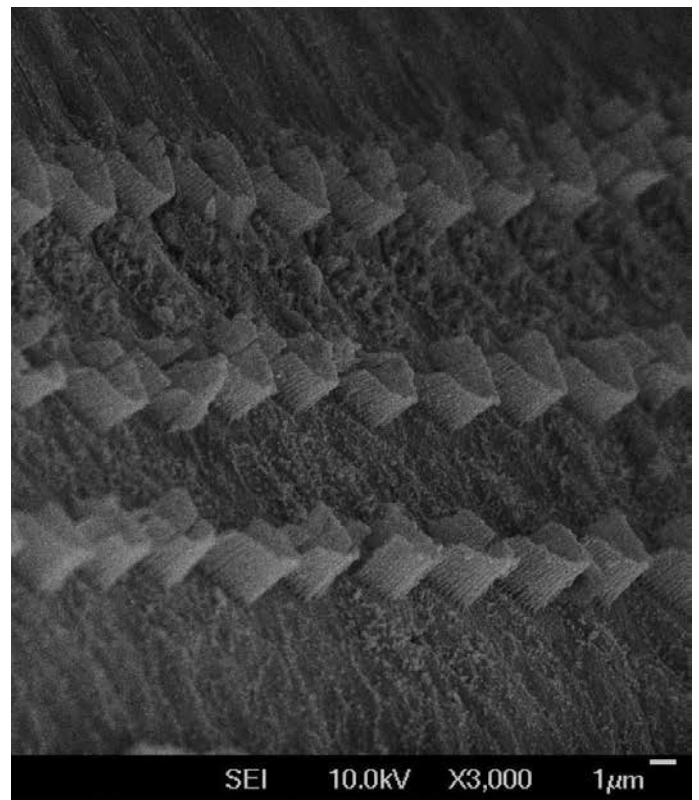

Figure 6. The surface topography of the organ of Corti in the control group: normal arrangement of OHC stereocilia.
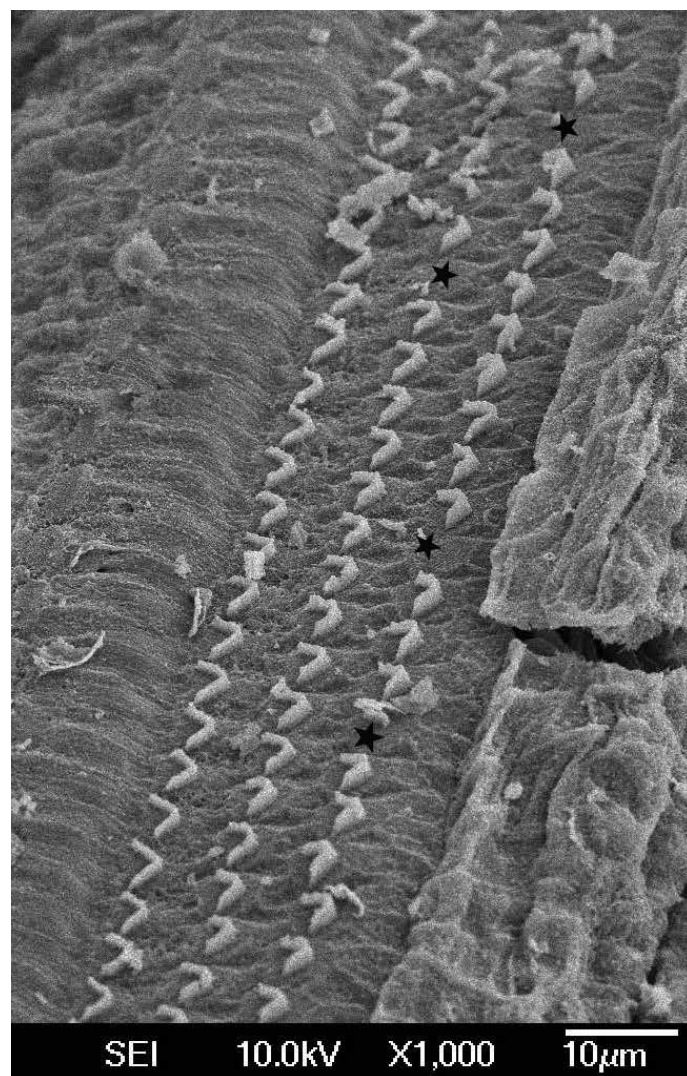OHC: outer hair cells

Figure 7. SEM micrograph depicting the surface topography of the organ of Corti in the G1 group: heterogeneously damaged OHC sterocilia.
OHC: outer hair cells; SEM: scanning electron microscopy
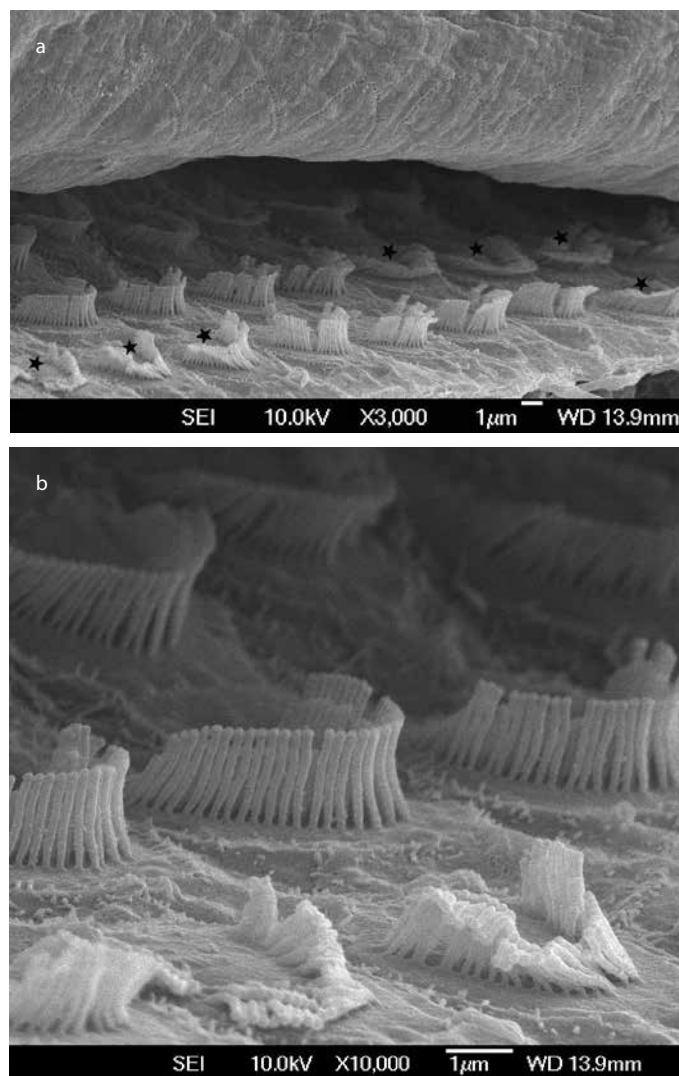

Figure 8. a, b. SEM micrograph: surface (a) and topographical (b) examinations of the organ of Corti in the G8 group reveal heterogeneously damaged OHC sterocilia.
OHC: outer hair cells; SEM: scanning electron microscopy

tribution of damaged cells was not regular and was not limited to a certain part of the basilar membrane.

DISCUSSION

In this study, we demonstrated the discrepancy between electrophysiological alterations and ultrastructural damage in the cochlea in the presence of pure-tone acoustic trauma. DPOAE recordings showed pure-tone hearing loss, whereas electron microscopy of the cochlea revealed heterogeneous damage of OHCs, rather than region-specific damage. Although the acoustic trauma affected other cochlear segments, degeneration on the trauma-generating frequency bands was more specific in DPOAE recordings. We expected damage of the areas corresponding to 1 and 8 kHz and intact segments on the basal membrane. In other words, OHC damage should be confined to the areas corresponding to these frequency bands. In contrast, there was widespread damage, i.e., damaged and intact OHCs together on the same segments of the basilar membrane. These findings challenge the traveling wave theory proposed by von Bekesy. Von Bekesy suggested that certain frequencies of sound vibrate at certain places on the basilar membrane and that frequency

discrimination is dependent on the passive movements/vibrations of the basilar membrane. If this claim was true, pure-tone acoustic stimuli would have led to OHC damage on places where the maximal wave amplitude occurs. On the contrary, the OHC damage was widespread and heterogeneous following high-intensity pure-tone acoustic stimuli (1 and 8 kHz in this study). The damage of 1 and 8 kHz trauma was comparable. In other words, the electrophysiological examination showed different types of hearing loss, i.e., 1 versus 8 kHz hearing loss, whereas the electron microscopic examination revealed similar damage patterns.

In these tests, a response specific to the frequency of a stimulus given to the traumatized right ear was recorded from the left ear; however, amplitudes of these responses increased or decreased. These responses might be due to the ability of OHCs on the basilar membranes of different cochlear segments to create maximum and minimum amplitude responses. OHC motile responses were evaluated with SOAE, and the amplitude changed depending on the segmental damage to OHCs. These findings suggest that OHCs in the right ear were damaged, whereas IHCs were undamaged and that the IHCs

passed the sound information to left OHCs. Thus, it can be postulated that any sound from the ear and the frequency resolution are primarily taken by ipsilateral IHCs to be transferred to contralateral OHCs. Our electrophysiological findings suggested that pure-tone acoustic trauma leads to some cochlear-dead regions with which we are familiar with in some clinical conditions. However, ultrastructural findings did not support this idea.

There may be several possible mechanisms to explain our findings. OHCs exhibit different characteristics along the basilar membrane from the base to the apex. Morphologically, the height is increased toward the apex [4]. The phalangeal structures of Deiters' cells can support maximum and minimum OHC vibration points and cochlear amplification. Deiters' cells are similar in diameter, independent of the cell's position in the organ of Corti and along the cochlear spiral, with similar morphology on the basilar membrane. They are very stiff and lack the capacity for rapid movements, and we do not know the reason why OHCs and Deiters' cells form a unique angled arrangement and interlock with each other [12, 13]. If the basilar membrane was of primary importance and peak vibrations of a particular sound frequency were stimulating OHCs of corresponding region, OHCs would not be necessary to show the different features along the basilar membrane. The linear theory of hearing suggests that frequency discrimination induced by vibrations can be performed on cells of the same type in every region of the membrane. However, OHCs have different properties across the membrane, which suggests a primary role for them. Another feature is the sequences and settlements of OHCs on the basilar membrane; when three rows of OHCs of the basilar membrane settle, successive longitudinal cells are not in contact with each other. However, when we look at the order of IHCs, the lateral walls of these cells appear to be in contact with each other [4, 14, 15]. For a certain group of OHCs to resonate according to the vibration frequency, this isolation seems inevitable. Another feature of OHCs is the cochlear frequency-specific axis, with different molecular properties showing differences in voltage-sensitive channels [16]. As voltage sensors, OHCs emit frequency-specific responses with their structural motor proteins [17] and different motility responses with efferent stimulation [8]. This motor protein, prestin, is necessary for cochlear amplification and sharp frequency tuning [18, 19]. Xia et al. [13] used a noise exposure protocol to cause hair cell loss localized to the basal region of the cochlea, resulting in high-frequency hearing loss. This caused residual OHCs to increase their expression of prestin mRNA and protein. To maintain the stability of auditory thresholds and frequency discrimination, the cochlea increases prestin expression in regions where there is no OHC loss [13]. Recently, Lamas et al. [20] demonstrated that acoustic input and efferent activity regulate the expression of prestin at transcriptional and post-transcriptional levels. Another study showed that OHC-type II spiral ganglion neurons drive the MOCE reflex-mediated control of the cochlear amplifier [21].

The frequencies of waves emitted by the movement of the basilar membrane are different. At 30 dB SPL, peak reticular lamina movements are two-fold greater than those of the basilar membrane, a difference that becomes smaller as the stimulus level increases in a living cochlea [22]. Our findings in this study regarding the mobility of the reticular lamina may be an example. Waves emitted from the cochlea travel in a linear fashion. A linear cochlea, with its OHC motility, becomes non-linear in character; this feature has been shown in some studies [22, 23]. OHC motility is absent in the post-mortem period, which lacks cochlear amplification. The maximum contraction is ap-

proximately two times the displacement of the basilar membrane at 40 dB SPL; it decreases to approximately 0.8 at 90 dB SPL, and there is no phase or amplitude difference between the reticular lamina and basilar membrane in the post-mortem period [22]. This displacement found in the organ of Corti as a result of a fluid being pushed into it by motile OHCs is significant for motion amplification at low sound pressure levels [24]. Hearing starts in linear fashion (IHCs) and continues non-linearly (OHCs).

The motility of OHCs was first reported by Brownell in 1985 [25]. The exact function of the slow and fast types of motility and the possible role of the efferent control of motility are much researched topics. Almost all work on OHC motility uses in vitro measures of excised OHCs. No complete in vitro study has been conducted to fully explain how OHC motility operates in a normal living cochlea. However, the discovery of the motor protein prestin provides a clue as to the manner in which motility may exist at very high rates of sound stimulation. It seems clear that there is no longer a need to postulate some form of a second-filter mechanism to explain differences between the sensitivity and frequency selectivity measured along the basilar membrane and that measured in the auditory nerve (at least for mammals) [26]. Furthermore, according to the second filter model, the $2f_1-f_2$ combination tone is the major product generated by the model [27]. However, more recently, it has been shown that in the presence of contralateral acoustic stimulation, f_2-f_1 rather than $2f_1-f_2$ is significantly affected [28].

In conclusion, we demonstrated that electrophysiological alterations and ultrastructural damage in the presence of pure-tone acoustic trauma are not concordant. Furthermore, ultrastructural evaluation by SEM revealed that the damage of 1 versus 8 kHz pure-tone acoustic trauma was comparable. The damage was widespread, and there were damaged and intact OHCs together on the same segments of the basilar membrane. These findings challenge the traveling wave theory proposed by von Bekesy. We concluded that basilar membrane movement in the cochlear frequency discrimination of sound is not the primarily important factor. Rather, the neural information that is transferred from IHCs to OHCs and OHC electromotility that occurs due to efferent stimulation may be the primary responsible factor for frequency discrimination in the cochlea.

REFERENCES

1. Von Bekesy G. Simplified model to demonstrate the energy flow and formation of traveling waves similar to those found in the cochlea. Proc Nat Acad Sci 1956; 42: 930-44. [CrossRef]
2. Dong W, Olson ES. Detection of cochlear amplification and its activation. Biophys J 2013; 105: 1067-78. [CrossRef]
3. Gao SS, Wang R, Raphael PD, Moayedi Y, Groves AK, Jian ZY, et al. Vibration of the organ of Corti within the cochlear apex in mice. J Neurophysiol 2014; 112: 1192-204. [CrossRef]
4. Raphael Y, Altschuler RA. Structure and innervation of the cochlea. Brain Res Bull 2003; 60: 397-422. [CrossRef]
5. Karavitaki KD, Mountain DC. Evidence for outer hair cell driven oscillatory fluid flow in the tunnel of Corti. Biophys J 2007; 92: 3284-93. [CrossRef]
6. Dallos P, Falkler B. Prestin, a new type of motor protein. Nat Rev Mol Cell Biol 2002; 3: 104-11. [CrossRef]
7. Zheng J, Shen W, He ZZD, Long KB, Madison LD, Dallos P. Prestin is the motor protein of cochlear outer hair cells. Nature 2000; 405: 149-55. [CrossRef]
8. Guinan JJ. Olivocochlear Efferents; Anatomy, physiology, function, and the measurement of efferent effects in humans. Ear Hear 2006; 27: 589-607. [CrossRef]
9. Frelenkov GI. Regulation of electromotility in the cochlear outer hair cell. J Physiol 2006; 576: 43-8. [CrossRef]
10. Le CS, Avan P, Gilain L, Romand R. CD hearing impaired mice. I: distortion product otoacoustic emission levels, cochlear function and morphology. Hear Res 1998; 120: 37-50. [CrossRef]
11. Uzun C, Koten M, Adalı MK, Karasalihoğlu AR. Method of measuring transient evoked otoacoustic emissions in guinea pigs. Kulak Burun Bogaz Ihtis Derg 2000; 7: 97-105.
12. Arya P, Webster P, Kalinec F. Deiters cells tread a narrow path-The Deiters cells-basilar membrane junction. Hear Res 2012; 290: 13-20. [CrossRef]
13. Xia A, Song Y, Wang R, Gao SS, Clifton W, Raphael P, et al. Prestin regulation and function in residual outer hair cells after noise-induced hearing loss. PLoS One 2013; 8: 1-12. [CrossRef]
14. Santi PA, Tsuprun VL. Cochlear Microanatomy and Ultrastructure. In: AF. Jahn, JS-Sacchi, editors. Physiology of the Ear. 2nd ed. San Diego: Singular Thomson Learning; 2001. p. 257-81.
15. Slepecky NB. Structure of the Mammalian Cochlea. In: Dallos P, Popper AN, Fay RR, editors. The Cochlea. 1st ed. New York: Springer; 1996. p. 54-71. [CrossRef]
16. Engel J, Braig C, Rüttiger L, Kuhn S, Zimmermann U, Blin C, et al. Two classes of outer hair cells along the tonotopic axis of the cochlea. Neuroscience 2006; 143: 837-49. [CrossRef]
17. Liberman MC, Gao J, He DZ, Wu X, Jia S, Zuo J. Prestin is required for electromotility of the outer hair cell and for the cochlear amplifier. Nature 2002; 419: 300-4. [CrossRef]
18. Dallos P, Wu X, Cheatham MA, Gao J, Zheng J, Anderson CT, et al. Prestin-based outer hair cell motility is necessary for mammalian cochlear amplification. Neuron 2008; 58: 333-9. [CrossRef]
19. Dallos P. Cochlear amplification, outer hair cells and prestin. Curr Opin Neurobiol 2008; 18: 370-6. [CrossRef]
20. Lamas V, Arévalo JC, Juiz JM, Merchán MA. Acoustic input and efferent activity regulate the expression of molecules involved in cochlear micromechanics. Front Syst Neurosci 2015; 8: 253-8. [CrossRef]
21. Froud KE, Wong AC, Cederholm JM, Klugmann M, Sandow SL, Julien JP, et al. Type II spiral ganglion afferent neurons drive medial olivocochlear reflex suppression of the cochlear amplifier. Nat Commun 2015; 6: 7115-8. [CrossRef]
22. Zha D, Chen F, Ramamoorrthy S, Fridberger A, Choudhury N, Jacques SL, et al. In vivo outer hair cell length changes expose the active process in the cochlea. Plos One 2012; 7: 1-9. [CrossRef]
23. Rubles L, Ruggero M. Mechanics of the Mammalian Cochlea. Physiological Reviews 2001; 81: 1305-52.
24. Zagadou BF, Mountain DC. Analysis of the cochlear amplifier fluid pump hypothesis. JARO 2012; 13: 185-97. [CrossRef]
25. Brownell WE, Bader CR, Bertrand D, de Ribaupierre Y. Evoked mechanica responses of isolated cochlear outer hair cells. Science 1985; 227: 194-6. [CrossRef]
26. Yost WA. Fundamentals of Hearing: An introduction. 5th ed. Netherlands: Brill; 2013.p.119-20.
27. Duifhuis H. Cochlear nonlinearity and second filter: Possible mechanism and implications. J Acoust Soc Am 1976: 59; 408-23. [CrossRef]
28. Wittekindt A, Gaese BH, Kössl M. Influence of contralateral acoustic stimulation on the quadratic distortion product f2-f1 in humans. Hear Res 2009; 247: 27-33.[CrossRef]